

Characterization of a Class of Error Correcting Frames for Robust Signal Transmission over Wireless Communication Channels

Gagan Rath

*IRISA, INRIA, Campus de Beaulieu, 35042 Rennes, France
Email: gagan.rath@irisa.fr*

Christine Guillemot

*IRISA, INRIA, Campus de Beaulieu, 35042 Rennes, France
Email: christine.guillemot@irisa.fr*

Received 14 July 2003; Revised 24 May 2004

Joint source-channel coding has been introduced recently as an element of QoS support for IP-based wired and wireless multimedia. Indeed, QoS provisioning in a global mobility context with highly varying channel characteristics is all the most challenging and requires a loosening of the layer and source-channel separation principle. Overcomplete frame expansions have been introduced as joint source-channel codes for erasure channels, that is, to allow for a signal representation that would be resilient to erasures in wired and wireless channels. In this paper, we characterize a class of frames for error correction besides erasure recovery in such channels. We associate the frames with complex number codes and characterize them based on the BCH-like property of the parity check matrices of the associated codes. We show that, in addition to the BCH-type decoding, subspace-based algorithms can also be used to localize errors over such frame expansion coefficients. When the frame expansion coefficients are quantized, we modify these algorithms suitably and compare their performances in terms of the accuracy of error localization and the signal-to-noise ratio of the reconstructed signal. In particular, we compare the frames associated with lowpass DFT, DCT, and DST codes, which belong to the defined class, in terms of their error correction efficiency.

Keywords and phrases: frame theory, error correction, compression, block transforms, wireless communication.

1. INTRODUCTION

The development of “Beyond 3G” (B3G) or “4G” networks and applications with all-IP-based seamless and ubiquitous service provisioning across heterogeneous infrastructures presents a number of technological challenges. Providing IP-based audio and video communications at the same, or at least comparable, “carrier class” and bandwidth efficiency as the corresponding circuit-switched subsystems of 3G and 2G remains an issue to be solved. There is a growing awareness and understanding that efficient QoS provisioning in a global mobility context with highly varying channel characteristics (bandwidth, throughput, error rates, fading, and erasure characteristics, etc.) requires a loosening and a rethinking of the end-to-end and layer separation principle. In particular, it is becoming a common understanding that vertical cross-layer cooperation may be beneficial because of both of the error and erasure resilience capabilities of emerging coding technology and of the idiosyncrasies of the wireless links. Both the link layer including the radio bearer

system and the higher layers will indeed benefit from QoS-related information exchange.

The robust header compression (ROHC) framework [1], and the new UDP-Lite protocol—possibly delivering erroneous packets to the application layer [2]—are strong steps towards a loosening and a rethinking of the end-to-end and the layer separation principle. Situated between link and IP layers, the ROHC [1] framework addresses the problems of spectrum and bandwidth scarcity and of packet header corruption due to bit errors characterizing wireless links. The fact that, for some applications, erroneous packet payloads can be valuable and better to cope with than the lost ones, has inspired the introduction of the UDP-lite transport protocol [2]. Assuming ROHC, UDP-lite, and an appropriate inter- or cross-layer signaling mechanism in action, this paper considers a joint source-channel coding scheme in the application layer which is based on the use of a certain class of frames.

Overcomplete frame expansions have been introduced recently as a signal representation that would be resilient to erasures in wireless channels [3, 4]. Frames are sets of vectors

in a Hilbert space which span the space but may contain larger number of vectors than a basis. The redundancy inherent in a frame makes the expansion resilient to additive and quantization noise and imparts stability to reconstruction. Overcomplete frame expansions for providing robustness to erasures in communication networks can be regarded as joint source-channel codes.

In this paper, we characterize a class of discrete frames which can be used for error correction besides erasure recovery. We associate the frames with complex number codes [5] and characterize them based on the structure of the parity check matrices of the associated codes. The structure of the codes is a generalization of that of the BCH-DFT codes [6, 7, 8]. We show that there are also other codes such as the discrete cosine transform (DCT) [9] and the discrete sine transform (DST) codes which have the same structure. Unlike DFT codes, DCT and DST codes are neither cyclic nor BCH. However, we show that a BCH-like decoding algorithm can be applied to localize and decode errors in such codes. We stress on the frame-theoretic formulation rather than the coding-theoretic approach because the codevectors need to be quantized before being transmitted. Introduction of quantization leads to errors beyond the error correcting capability of the codes and thus makes the underlining theory inefficient. In this context, the frame theory comes in hand since it can analyze the reconstruction errors and study the usefulness of the particular frame.

The second contribution of the paper is the introduction of subspace algorithms for localizing errors in the frame expansion coefficients. Subspace methods are popular in the direction of arrival (DOA) estimation [10, 11] and they can be applied to localize errors in DFT codes [12]. Here the subspace methods are extended to the generalized codes case. In the case of DFT codes, the locations of errors correspond to discrete frequencies and, therefore, the adaptation of subspace algorithms [12] seem straightforward. However, for the generalized codes defined here, the locations of errors may not correspond to any frequency, and hence the application of subspace methods is not so obvious. The motivation for introducing subspace methods is to increase the localization accuracy of errors when the coefficients are quantized. We compare the performances of the proposed subspace algorithm and the BCH decoding with lowpass DFT, DCT, and DST frames when they are used for transmitting a Gauss-Markov source and images.

2. FINITE FRAMES REVISITED

Consider the K -dimensional Euclidean complex space, that is, \mathbb{C}^K . A set of K -dimensional vectors $\Phi_G \equiv \{\varphi_k\}_{k=1}^N$ is called a frame if there exist $B_1 > 0$ and $B_2 < \infty$ such that

$$B_1 \|\mathbf{x}\|^2 \leq \sum_{k=1}^N |\langle \mathbf{x}, \varphi_k \rangle|^2 \leq B_2 \|\mathbf{x}\|^2, \quad \forall \mathbf{x} \in \mathbb{C}^K, \quad (1)$$

where $\langle \mathbf{x}, \varphi_k \rangle$ denotes the inner product of \mathbf{x} and φ_k , and $\|\mathbf{x}\|$ denotes the Euclidean norm of \mathbf{x} [4]. B_1 and B_2 are called the frame bounds. The inner product $\langle \mathbf{x}, \varphi_k \rangle$ gives the k th frame

expansion coefficient of \mathbf{x} . Any finite set of vectors that spans \mathbb{C}^K is a frame. Therefore a frame will always have $N \geq K$. The ratio N/K is normally referred to as the redundancy of the frame. The frame Φ_G is associated with a frame operator G which is defined as follows:

$$(G\mathbf{x})_k \equiv \langle \mathbf{x}, \varphi_k \rangle, \quad \text{for } k = 1, 2, \dots, N. \quad (2)$$

Thus the frame expansion coefficients of \mathbf{x} are given by $G\mathbf{x}$. A frame is called *tight* if its bounds are equal, that is, $B_1 = B_2$. Hence Φ_G is tight if and only if $G^h G = BI_K$, where $B = B_1 = B_2$. This implies that the columns of G are orthogonal. A frame is called *normalized* or *uniform* if each frame vector has length equal to 1 [4]. Associated with the frame Φ_G , there exists a dual frame whose frame operator is given as $\tilde{G} = G(G^h G)^{-1}$. Given the frame expansion coefficients of any vector \mathbf{x} , the vector can be reconstructed using the dual frame operator as $\hat{\mathbf{x}} = \tilde{G}^h(G\mathbf{x})$. The conjugate transpose of the dual frame operator is the pseudoinverse of the frame operator, and it minimizes the reconstruction error [4]. For details about frame theory and signal representation with overcomplete sets, the reader is referred to [13].

3. ERROR CORRECTING FRAMES

Frames provide redundant representations of signals. The redundancy of the representation can be utilized for various purposes such as providing stable reconstructions, enhancing the quality of the reconstructions, and providing robustness against additive noises. Recently frames have been proposed for use in communication channels for providing robustness to erasures [3, 4]. Even if some of the frame expansion coefficients are lost during the transmission, the message signal can still be reconstructed from the received coefficients. In addition, the quality of the reconstruction improves as the number of lost coefficients decreases. This is contrary to the case with classical critical representation of a signal when the loss of a coefficient cannot be recovered without the help of error control coding.

The frames used for providing robustness to erasures must possess certain desired properties. For example, with a frame expansion in \mathbb{C}^K , in order to reconstruct the message with any K received coefficients, the set of frame vectors associated with the received coefficients must also be a frame [4]. Further, in order to minimize the reconstruction error due to quantization of the coefficients, this frame must be tight [4]. Not all frames do possess these properties. In the following we characterize a class of frames which cannot only recover erased coefficients but also correct additive errors in frame coefficients.

Consider the frame Φ_G . It is associated with an (N, K) complex block code whose generator matrix is the frame operator G . Since the frame vectors span \mathbb{C}^K , the columns of G are linearly independent and they define a subspace which is the codespace associated with the frame Φ_G . A parity check matrix of the code, denoted by H , can be obtained from the singular value decomposition (SVD) of G . Let the SVD of G

be given as

$$G = V_1 \Sigma V_2^h, \quad (3)$$

where V_1 is an $N \times N$ unitary matrix, V_2 is a $K \times K$ unitary matrix, and Σ is an $N \times K$ matrix having $N - K$ null row vectors. H can be obtained by taking those columns of V_1 which have the same indices as those of the null row vectors of Σ . Since V_1 is unitary, the columns of H are linearly independent and $H^h G = \mathbf{0}_{(N-K) \times K}$.

Notice that, in the frame-theoretic formulation, the rows of the matrix G are the basic elements; they form a spanning set for a K -dimensional space. This is in contrast with the coding-theoretic formulation where the columns of the matrix G are the basic elements; they form a basis for a K -dimensional subspace of an N -dimensional space. For a given message vector, the vector of frame expansion coefficients and the codevector are one and the same.

The number of complex errors that this frame can detect and correct depends on the minimum distance of the associated code. The Hamming distance between two codewords is defined as the number of positions or indices in which they differ from each other [5]. In the following, we characterize a class of codes which are BCH-like: their parity check matrices have similar properties as those of BCH codes so that a BCH decoding algorithm can be applied to correct errors. This will equivalently characterize a class of frames which are associated with those codes. We consider the "errors only" case here since the extension to errors with erasures is straightforward.

3.1. BCH-like complex codes

For notational convenience, we set $d = N - K$, where d is a positive integer. Let there be d complex polynomials $p_1(x), p_2(x), \dots, p_d(x)$ of order $d-1$ each, where the i th polynomial is defined as

$$p_i(x) = a_{i1} + a_{i2}x + \dots + a_{id}x^{d-1}. \quad (4)$$

Let the polynomials be such that the coefficient matrix A , which is given as

$$A \equiv \begin{bmatrix} a_{11} & a_{12} & \dots & a_{1d} \\ a_{21} & a_{22} & \dots & a_{2d} \\ \vdots & \vdots & \ddots & \vdots \\ a_{d1} & a_{d2} & \dots & a_{dd} \end{bmatrix}, \quad (5)$$

is nonsingular. Let f be a one-to-one nonzero complex function defined on the index set $\{0, 1, \dots, N-1\}$. Let the elements of H^h be specified as $h_{ij} = u_j p_i(f(j-1))$, $1 \leq i \leq d$, $1 \leq j \leq N$, where u_1, \dots, u_N are nonzero scalars. Then H is a parity check matrix of a maximum distance separable (MDS) complex code. Such a code can correct up to $\lfloor d/2 \rfloor$ errors and can recover up to d erasures.

To prove the above assertion, we see that the conjugate transpose of the parity check matrix can be expressed as

$$H^h = AXU, \quad (6)$$

where X is $d \times N$ with i th column equal to $[1, f(i-1), \dots, f^{d-1}(i-1)]^t$ and U is a diagonal matrix with the i th diagonal entry equal to u_i . Since f is one-to-one and nonzero, any k , $k \leq d$, columns of X are linearly independent. As a result, any k , $k \leq d$, columns of H are also linearly independent. Therefore the minimum distance of the code is $d+1$ and the code is MDS [5].

3.2. Examples

3.2.1. DFT codes

An (N, K) DFT code is a linear block code whose generator matrix consists of any K columns from the inverse DFT matrix of order N [6]. A parity check matrix of the code consists of the remaining $N - K$ columns of the inverse DFT matrix. Since the DFT matrix is unitary, the frames associated with DFT codes are tight. If the parity frequencies are spaced by α , where α is relatively prime to N , then the DFT code is a BCH code in the complex field [6]. Let the parity frequencies be denoted by $0, \alpha, \dots, (d-1)\alpha$. Then the conjugate transpose of the parity check matrix is given as

$$H_f^h = \begin{bmatrix} 1 & 1 & \dots & 1 \\ 1 & w^\alpha & \dots & w^{(N-1)\alpha} \\ \vdots & \vdots & \ddots & \vdots \\ 1 & w^{(d-1)\alpha} & \dots & w^{(d-1)(N-1)\alpha} \end{bmatrix}, \quad (7)$$

where $w = e^{-j2\pi/N}$. It is easy to see that H_f^h has a similar structure as that of H^h with $X = H_f^h$, $A = I_d$, and $U = I_N$. I_d and I_N denote identity matrices of order d and N , respectively. Clearly, the function f is defined as $f(i) = w^{i\alpha}$, $0 \leq i \leq N-1$. Real BCH-DFT codes are special cases of complex BCH-DFT codes [6]. If the parity frequencies of a complex BCH-DFT code are such that the complex conjugate of every column of the generator matrix also belongs to it, then, through elementary column operations, the DFT code can be made real. For example, a real BCH-DFT code is defined by the following generator matrix [7, 8, 14, 15]:

$$G = \sqrt{\frac{N}{K}} W_N^h \Sigma W_K, \quad (8)$$

where W_K is the DFT matrix of order K , W_N^h is the conjugate transpose of the DFT matrix of order N , and Σ is an $N \times K$ binary matrix with 1's given as $\Sigma_{00} = 1$, $\Sigma_{ii} = \Sigma_{N-i, K-i} = 1$, for $i = 1, \dots, (K-1)/2$. Here K is assumed to be odd. For this code, the parity check matrix is given by

$$H_f^h = XU, \quad (9)$$

where

$$X = \begin{bmatrix} 1 & 1 & \dots & 1 \\ 1 & w & \dots & w^{(N-1)} \\ \vdots & \vdots & \ddots & \vdots \\ 1 & w^{(d-1)} & \dots & w^{(d-1)(N-1)} \end{bmatrix}, \quad (10)$$

and U is a diagonal matrix with the i th diagonal entry equal to $w^{((K+1)/2)i}$, $i = 0, \dots, N-1$. Obviously, here $A = I_d$ and the function f is given as $f(i) = w^i$, $0 \leq i \leq N-1$. Since the parity frequencies correspond to the high-frequency indices, this code can also be termed as a lowpass code [6]. We can have similar formulation for a highpass DFT code.

3.2.2. DCT codes

An (N, K) DCT code is a linear block code whose generator matrix consists of any K columns from the inverse DCT matrix of order N [9]. Here we use the inverse DCT matrix in order to be consistent with the definition of DFT codes. A parity check matrix of the code consists of the remaining $N-K$

columns of the inverse DCT matrix. DCT codes are real block codes. Since the DCT matrix is orthogonal, the frames associated with DCT codes are tight. Consider the DCT code whose parity frequencies correspond to the highest $N-K$ frequencies. Here we consider the type-II DCT matrix whose (i, j) th element is given as

$$\theta(i, j) = \sqrt{\frac{2}{N}} \alpha(i) \cos \frac{(2j+1)i\pi}{2N}, \quad 0 \leq i, j \leq N-1, \quad (11)$$

$$\alpha(0) = \frac{1}{\sqrt{2}}, \quad \alpha(i) = 1, \quad i \neq 0.$$

The parity check matrix of this code can be given as

$$H_c^t = \begin{bmatrix} \cos \frac{(N-d)\pi}{2N} & \cos \frac{(N-d)3\pi}{2N} & \cdots & \cos \frac{(N-d)(2N-1)\pi}{2N} \\ \vdots & \vdots & \vdots & \vdots \\ \cos \frac{(N-2)\pi}{2N} & \cos \frac{(N-2)3\pi}{2N} & \cdots & \cos \frac{(N-2)(2N-1)\pi}{2N} \\ \cos \frac{(N-1)\pi}{2N} & \cos \frac{(N-1)3\pi}{2N} & \cdots & \cos \frac{(N-1)(2N-1)\pi}{2N} \end{bmatrix}. \quad (12)$$

By rearranging the rows in reverse order and using basic trigonometric relations, it can be expressed as

$$H_c^t = \begin{bmatrix} \sin \frac{\pi}{2N} & -\sin \frac{3\pi}{2N} & \cdots & (-1)^{N-1} \sin \frac{(2N-1)\pi}{2N} \\ \sin \frac{2\pi}{2N} & -\sin \frac{6\pi}{2N} & \cdots & (-1)^{N-1} \sin \frac{(2N-1)2\pi}{2N} \\ \vdots & \vdots & \vdots & \vdots \\ \sin \frac{d\pi}{2N} & -\sin \frac{3d\pi}{2N} & \cdots & (-1)^{N-1} \sin \frac{(2N-1)d\pi}{2N} \end{bmatrix}. \quad (13)$$

Using the identity [16]

$$\sin(n\beta) = \sin\beta \left\{ (2\cos\beta)^{n-1} - \binom{n-2}{1} (2\cos\beta)^{n-3} + \binom{n-3}{2} (2\cos\beta)^{n-5} - \cdots \right\}, \quad (14)$$

this can be factorized as

$$H_c^t = AXU, \quad (15)$$

where

$$A = \begin{bmatrix} 1 & & & & \\ 0 & 2 & & & \\ -1 & & 0 & 4 & \\ \vdots & \ddots & & \ddots & \ddots \\ \cdots & & -(d-2)2^{d-3} & 0 & 2^{d-1} \end{bmatrix}_{d \times d},$$

$$X = \begin{bmatrix} 1 & 1 & \cdots & 1 \\ \cos \frac{\pi}{2N} & \cos \frac{3\pi}{2N} & \cdots & \cos \frac{(2N-1)\pi}{2N} \\ \vdots & \vdots & \vdots & \vdots \\ \cos^{d-1} \frac{\pi}{2N} & \cos^{d-1} \frac{3\pi}{2N} & \cdots & \cos^{d-1} \frac{(2N-1)\pi}{2N} \end{bmatrix}, \quad (16)$$

and U is a diagonal matrix with i th diagonal entry $(-1)^i \times \sin(2i+1)\pi/2N$, $i = 0, \dots, N-1$. A is a lower triangular nonsingular matrix. Obviously, the function f is given as $f(i) = \cos(2i+1)\pi/2N$, $0 \leq i \leq N-1$. Therefore, the above DCT code is BCH-like and can correct up to $\lfloor d/2 \rfloor$ errors. This is a lowpass DCT code since the parity frequencies are the higher frequencies. We can similarly have a highpass DCT code which is BCH-like. Note that, unlike DFT codes,

if the parity frequencies are spaced by α , where α is relatively prime to N , the DCT code may not be BCH-like because A may not be nonsingular.

3.2.3. DST codes

An (N, K) DST code is a linear block code whose generator matrix consists of any K columns from the inverse DST matrix of order N . A parity check matrix of the code consists of the remaining $N - K$ columns of the inverse DST matrix. Like DCT codes, DST codes are real block codes. The frames associated with the DST codes are also tight. Consider the DST

code whose parity frequencies are the highest $N - K$ frequencies. Here we consider the type-II DST matrix whose (i, j) th element is given as

$$\begin{aligned} \theta(i, j) &= \sqrt{\frac{2}{N}} \alpha(i) \sin \frac{(2j+1)(i+1)\pi}{2N}, \quad 0 \leq i, j \leq N-1, \\ \alpha(N-1) &= \frac{1}{\sqrt{2}}, \quad \alpha(i) = 1, \quad i \neq N-1. \end{aligned} \quad (17)$$

The parity check matrix can be given as

$$H_s^t = \begin{bmatrix} \sin \frac{(N-d+1)\pi}{2N} & \sin \frac{(N-d+1)3\pi}{2N} & \cdots & \sin \frac{(N-d+1)(2N-1)\pi}{2N} \\ \vdots & \vdots & \vdots & \vdots \\ \sin \frac{(N-1)\pi}{2N} & \sin \frac{(N-1)3\pi}{2N} & \cdots & \sin \frac{(N-1)(2N-1)\pi}{2N} \\ \frac{1}{\sqrt{2}} \sin \frac{\pi}{2} & \frac{1}{\sqrt{2}} \sin \frac{3\pi}{2} & \cdots & \frac{1}{\sqrt{2}} \sin \frac{(2N-1)\pi}{2} \end{bmatrix}. \quad (18)$$

By rearranging the rows in reverse order, the matrix can be

expressed as

$$H_s^t = \begin{bmatrix} \frac{1}{\sqrt{2}} & -\frac{1}{\sqrt{2}} & \cdots & (-1)^{N-1} \frac{1}{\sqrt{2}} \\ \cos \frac{\pi}{2N} & -\cos \frac{3\pi}{2N} & \cdots & (-1)^{N-1} \cos \frac{(2N-1)\pi}{2N} \\ \vdots & \vdots & \vdots & \vdots \\ \cos \frac{(d-1)\pi}{2N} & -\cos \frac{3(d-1)\pi}{2N} & \cdots & (-1)^{N-1} \cos \frac{(2N-1)(d-1)\pi}{2N} \end{bmatrix}. \quad (19)$$

Using the identity [16]

$$\begin{aligned} \cos(n\beta) &= \frac{1}{2} \left\{ (2 \cos \beta)^n - n(2 \cos \beta)^{n-2} \right. \\ &\quad \left. + \frac{n}{2} \binom{n-3}{1} (2 \cos \beta)^{n-4} - \cdots \right\}, \end{aligned} \quad (20)$$

this can be factorized as

$$H_s^t = AXU, \quad (21)$$

where

$$A = \begin{bmatrix} \frac{1}{\sqrt{2}} & & & & \\ 0 & 1 & & & \\ -1 & 0 & 2 & & \\ \vdots & \ddots & \ddots & \ddots & \\ \cdots & -(d-1)2^{d-4} & 0 & & 2^{d-2} \end{bmatrix}, \quad (22)$$

U is a diagonal matrix with i th diagonal entry $(-1)^i$, $i = 0, \dots, N-1$, and X is as defined for the lowpass DCT code.

A is a lower triangular nonsingular matrix. Therefore the above DST code is BCH-like and can correct up to $\lfloor d/2 \rfloor$ errors. This is a lowpass DST code since the parity frequencies are the higher frequencies. We can similarly have a highpass BCH-like DST code whose parity frequencies correspond to the low-frequency indices. Similar to DCT codes, parity frequencies spaced by α , where α is relatively prime to N , may not result in a BCH-like DST code.

4. DECODING OF ERRORS WITH UNQUANTIZED FRAME EXPANSIONS

The class of complex codes defined in the previous section is a generalization of the complex BCH codes. In the special case when $A = I_d$ and $U = I_N$, they are BCH. It is easy to see that the DFT codes defined by the parity check matrix H_f^h are BCH whereas the DCT and the DST codes are not BCH. In fact, the DCT and the DST codes are not even cyclic. Nevertheless, the BCH decoding algorithm can still be applied to decode the errors provided the number of erroneous coefficients is less than or equal to $\lfloor d/2 \rfloor$. In the following, we first present a syndrome decoding algorithm which is analogous to the syndrome decoding algorithm for complex BCH codes [17]. Then we present a subspace-based algorithm which follows the lines of MUSIC algorithm for DOA estimation in array signal processing.

4.1. Syndrome decoding

Let \mathbf{r} denote the received vector of coefficients when the actual coefficient vector \mathbf{y} is corrupted by the error vector \mathbf{e} . Hence $\mathbf{r} = \mathbf{y} + \mathbf{e}$. We assume that \mathbf{e} has ν nonzero components where $\nu \leq \lfloor d/2 \rfloor$. The syndrome of the received vector is given as

$$\mathbf{s} = H^h \mathbf{r} = H^h (\mathbf{y} + \mathbf{e}) = H^h \mathbf{e}, \quad (23)$$

where $\mathbf{s} \equiv [s(1), s(2), \dots, s(d)]^t$. Substituting the expression for H^h , we get

$$\mathbf{s} = AXU\mathbf{r}, \quad \text{or} \quad XU\mathbf{r} = A^{-1}\mathbf{s} \equiv \mathbf{z}, \quad (24)$$

where $\mathbf{z} \equiv [z(1), z(2), \dots, z(d)]^t$ denotes the modified syndrome vector. Recall that A is invertible by definition. Since $\mathbf{r} = \mathbf{y} + \mathbf{e}$, we get

$$XU(\mathbf{y} + \mathbf{e}) = XU\mathbf{e} = \mathbf{z}. \quad (25)$$

The above relation follows since XU is also a parity check matrix for the same code resulting in $XU\mathbf{y} = \mathbf{0}_{d \times 1}$.

Let d be equal to $2l$ or $2l + 1$ for some positive integer l if it is even or odd, respectively. Hence $\nu \leq l$. Let i_1, i_2, \dots, i_ν denote the indices of the erroneous coefficients. Let $X_k \equiv f(i_k)$, $k = 1, \dots, \nu$, and let e_k and U_k denote, respectively, the error in the coefficient having index i_k and the i_k th diagonal entry of U . Note the difference between u_k (k th diagonal entry of U) and U_k , and between X ($d \times N$ matrix with i th column $[1, f(i-1), \dots, f^{d-1}(i-1)]^t$, $0 \leq i \leq N-1$) and X_k , $k = 1, \dots, \nu$. Since the components of \mathbf{e} are equal to zero

at the indices of nonerroneous coefficients, (25) can be expanded as

$$\begin{bmatrix} 1 & 1 & \cdots & 1 \\ X_1 & X_2 & \cdots & X_\nu \\ \vdots & \vdots & \vdots & \vdots \\ X_1^{d-1} & X_2^{d-1} & \cdots & X_\nu^{d-1} \end{bmatrix} \begin{bmatrix} e_1 U_1 \\ e_2 U_2 \\ \vdots \\ e_\nu U_\nu \end{bmatrix} = \begin{bmatrix} z(1) \\ z(2) \\ \vdots \\ z(d) \end{bmatrix}. \quad (26)$$

Let S denote the modified syndrome matrix defined as

$$S \equiv \begin{bmatrix} z(1) & z(2) & \cdots & z(d-l) \\ z(2) & z(3) & \cdots & z(d-l+1) \\ \vdots & \vdots & \vdots & \vdots \\ z(l+1) & z(l+2) & \cdots & z(d) \end{bmatrix}. \quad (27)$$

Using (26), S can be factorized as $S = V_e D V_2^t$, where

$$V_e \equiv \begin{bmatrix} 1 & 1 & \cdots & 1 \\ X_1 & X_2 & \cdots & X_\nu \\ \vdots & \vdots & \vdots & \vdots \\ X_1^l & X_2^l & \cdots & X_\nu^l \end{bmatrix}, \quad D \equiv \begin{bmatrix} e_1 U_1 & & & \\ & \ddots & & \\ & & & e_\nu U_\nu \end{bmatrix},$$

$$V_2 \equiv \begin{bmatrix} 1 & 1 & \cdots & 1 \\ X_1 & X_2 & \cdots & X_\nu \\ \vdots & \vdots & \vdots & \vdots \\ X_1^{d-l-1} & X_2^{d-l-1} & \cdots & X_\nu^{d-l-1} \end{bmatrix}. \quad (28)$$

Since X_i 's are distinct and $\nu \leq l$, the columns of V_e are linearly independent and the columns of V_2 are also linearly independent. Therefore the rank of S is ν . This means that the number of coefficient errors can be found from the rank of S , or equivalently, by finding the order of the largest nonsingular submatrix of S .

Let $\Lambda(x)$ denote the error locator polynomial defined as

$$\Lambda(x) \equiv \prod_{i=1}^{\nu} (1 - X_i x^{-1}) = \Lambda_0 + \Lambda_1 x^{-1} + \cdots + \Lambda_\nu x^{-\nu}, \quad (29)$$

where $\Lambda_0 = 1$. We assert that the coefficients of the error locator polynomial satisfy the following set of equations:

$$z(j)\Lambda_\nu + z(j+1)\Lambda_{\nu-1} + \cdots + z(\nu+j)\Lambda_0 = 0, \quad (30)$$

$$j = 1, \dots, d - \nu.$$

To prove the assertion, from (26) we get $z(j) = \sum_{k=1}^{\nu} e_k U_k X_k^{j-1}$, $j = 1, \dots, d$. Substituting in the left-hand sides of the above equations and then rearranging the terms, we get

$$e_1 U_1 X_1^{j-1} \sum_{k=0}^{\nu} \Lambda_{\nu-k} X_1^k + e_2 U_2 X_2^{j-1} \sum_{k=0}^{\nu} \Lambda_{\nu-k} X_2^k$$

$$+ \cdots + e_\nu U_\nu X_\nu^{j-1} \sum_{k=0}^{\nu} \Lambda_{\nu-k} X_\nu^k. \quad (31)$$

This can be further simplified as

$$\begin{aligned}
 & e_1 U_1 X_1^{\nu+j-1} \sum_{k=0}^{\nu} \Lambda_k X_1^{-k} + e_2 U_2 X_2^{\nu+j-1} \sum_{k=0}^{\nu} \Lambda_k X_2^{-k} \\
 & + \cdots + e_{\nu} U_{\nu} X_{\nu}^{\nu+j-1} \sum_{k=0}^{\nu} \Lambda_k X_{\nu}^{-k}.
 \end{aligned} \tag{32}$$

Since X_i 's are the roots of $\Lambda(x)$, the summation terms are equal to zero, and hence the sum of the terms is zero. Conversely, it is easy to see that the solutions of (30) are the error locator polynomial coefficients whose roots are X_i 's.

Equation (30) is similar to the convolution relation between the syndrome coefficients and the locator polynomial coefficients in the case of DFT codes [5, 18]. In the latter, the equations can also be derived from the relationship between the error vector \mathbf{e} and the inverse DFT of $\mathbf{\Lambda} \equiv [\Lambda_0, \Lambda_1, \dots, \Lambda_{\nu}, \mathbf{0}_{1 \times (N-1-\nu)}]$. The elementwise multiplication of \mathbf{e} and the inverse DFT of $\mathbf{\Lambda}$ is equal to the null vector, and hence the circular convolution of $\mathbf{\Lambda}$ and the DFT of \mathbf{e} is also a null vector. The DFT of \mathbf{e} over the parity frequencies gives the syndrome, and hence the relationship follows. Here the same relationship holds for the defined generalized case. Now these equations can be solved for the locator polynomial coefficients through matrix inversion [17] or iterative schemes [17, 18]. The roots of the error locator polynomial give X_i 's, and the inverse mapping f^{-1} finds the indices of the erroneous coefficients. Since the number of equations in (30) is $d - \nu$, the maximum number of errors that can be localized is equal to l . Once the errors are localized, their magnitudes can be determined by solving the first ν syndrome equations in (23), or equivalently, by solving the first ν modified syndrome equations in (26).

4.2. A subspace decoding approach

Subspace-based algorithms such as the MUSIC, the minimum-norm method, and the ESPRIT are very popular for estimating the DOAs of plane waves in array signal processing [10]. The basic idea in those algorithms is to estimate the signal subspace and its orthogonal complement, the noise subspace, from the eigendecomposition of the data covariance matrix. Usually, the received data is corrupted by some background noise which is assumed to be white. Here we first develop an error localization algorithm which is based on the subspace concept but without the presence of quantization noise. The decoding algorithm for quantized coefficients, which is similar to the classical MUSIC, is developed in Section 5.2.2. Earlier we have shown that analogous subspace algorithms can be developed to localize sample errors in DFT codes [12]. They localize errors with better accuracy due to the higher degrees of freedom associated with the subspaces [12]. In the following, we develop the subspace algorithm for the class of frames defined in the previous section along the same line. Though the development looks apparently the same as those for DFT codes, the generalized structure of the defined class must be borne in mind. In the case of DFT codes, the syndrome coefficients are sums of complex sinusoids whose

frequencies are determined by the error locations. For the class of codes defined here, the syndrome depends on the matrices A , U , and the function f , and hence the error localization may not have an interpretation of frequency estimation. For the convenience of understanding, we have used the same notations for error locator vectors, syndrome matrix, eigenvectors, and so forth, as in [12].

Consider the matrix V_e whose i th column is $[1, X_i, \dots, X_i^{l-1}]^t$, $i = 1, \dots, \nu$ (refer to the factorization of modified syndrome matrix S). Since X_i 's determine the error locations, we will refer to the columns of V_e as the error locator vectors and to V_e as the error locator matrix. Since X_i 's are distinct and $\nu < l + 1$, the error locator vectors are linearly independent. They define a ν -dimensional subspace of the $(l + 1)$ -dimensional vector space, which we will refer to as the channel error subspace. The orthogonal complement of this subspace has dimension $l + 1 - \nu$, and we will refer to it as the noise subspace.

Let $R \equiv (1/(d-l))SS^h$. We will refer to R as the syndrome covariance matrix. Since the rank of S is ν , the number of sample errors, the rank of R is also equal to ν . Therefore it has ν nonzero eigenvalues. The eigenvalues are all real since R is Hermitian. The eigendecomposition of R can be given as

$$R = \begin{bmatrix} U_e^{(l+1) \times \nu} & U_n^{(l+1) \times (l+1-\nu)} \end{bmatrix} \begin{bmatrix} \Delta_e^{\nu \times \nu} & \mathbf{0} \\ \mathbf{0} & \mathbf{0}_{(l+1-\nu) \times (l+1-\nu)} \end{bmatrix} \begin{bmatrix} U_e & U_n \end{bmatrix}^h, \tag{33}$$

where Δ_e contains the nonzero eigenvalues, U_e contains the eigenvectors corresponding to the nonzero eigenvalues, and U_n contains the eigenvectors corresponding to the eigenvalue zero. Note that the notations here have no relations with the $N \times N$ diagonal matrix U defined in Section 3.1 for characterizing the frames. The following proposition establishes the relationship between the eigenvectors of R and the error locator vectors.

Proposition 1. *The columns of U_e span the channel error subspace.*

This proposition can be proved using a similar method as for DFT codes [12].

Because of this result, the error locator vectors are orthogonal to the eigenvectors in U_n , which span the noise subspace. That is, $V_e^h U_n = \mathbf{0}_{\nu \times (l+1-\nu)}$. Let $\Phi_i(x)$ denote the polynomial associated with the i th column of U_n . From the above orthogonality relation, it follows that X_1^*, \dots, X_{ν}^* are common roots of $\Phi_1(x), \dots, \Phi_{l+1-\nu}(x)$. Further, since $\nu < l + 1$, they are the only common roots. For DCT and DST frames, $X_i^* = X_i$, because the function $f(i)$ is real. Therefore the errors are localized by finding the common roots of the polynomials $\Phi_i(x)$ and then applying the inverse mapping f^{-1} . The common roots can be determined by finding the zeros of the following function over the range of f :

$$E(x) \equiv \mathbf{v}_x^h U_n U_n^h \mathbf{v}_x, \tag{34}$$

where $\mathbf{v}_x \equiv [1, x, x^2, \dots, x^{l-1}]^t$.

It is obvious that both the syndrome decoding and the subspace decoding produce perfect error localizations so long as there is no quantization and the number of coefficient errors is less than or equal to $\lfloor d/2 \rfloor$. In fact, it can be shown that the minimum-norm vector lying in the noise subspace is nothing but the vector consisting of the error locator polynomial coefficients appended by $(l - \nu)$ zeros, that is, $\Lambda_l \equiv [1, \Lambda_1, \dots, \Lambda_\nu, \overbrace{0, \dots, 0}^{l-\nu}]^t$ [12]. Observe that the syndrome matrix dimension can be any of $m \times (d - m + 1)$, $\nu + 1 \leq m \leq d - \nu + 1$, so that the error subspace has dimension ν and the noise subspace has dimension at least 1. However, we have observed that taking m equal to $l + 1$ produces the best localization results when the coefficients are quantized. Therefore, we have chosen m to be equal to $l + 1$. When the number of coefficient errors is equal to l , the noise subspace has dimension equal to one, and, in this case, the single-column vector in U_n is the normalized Λ_l .

5. DECODING OF QUANTIZED FRAME EXPANSIONS

The transmission of the frame expansion coefficients in a digital form requires all coefficients to be quantized. As a result, every coefficient vector contains N coefficient errors irrespective of any channel error. Therefore the decoding algorithms described in the previous section cannot be applied directly in order to correct the errors. The problem of error correction now becomes a problem of estimation. The decoding algorithms will aim at localizing and finding the channel errors having large magnitudes compared to the quantization noise.

Let \mathbf{q} denote the quantization noise of coefficient vector \mathbf{y} . With channel error \mathbf{e} , the received vector is given as $\hat{\mathbf{r}} = \mathbf{y} + \mathbf{q} + \mathbf{e}$. We will denote the terms defined earlier with a hat to indicate the presence of quantization noise. Therefore the syndrome is given as

$$\hat{\mathbf{s}} = H^h \hat{\mathbf{r}} = H^h \mathbf{q} + H^h \mathbf{e} = \mathbf{s}_q + \mathbf{s}_e, \quad (35)$$

where $\mathbf{s}_q \equiv H^h \mathbf{q}$ and $\mathbf{s}_e \equiv H^h \mathbf{e}$. It is easy to see that \mathbf{s}_q denotes the contribution of the quantization noise to the syndrome. Therefore a nonzero syndrome does not imply the presence of channel errors. Note that the receiver can compute $\hat{\mathbf{s}}$, but not \mathbf{s}_q and \mathbf{s}_e since \mathbf{q} is not known. The modified syndrome can be computed analogously as $\hat{\mathbf{z}} = A^{-1} \hat{\mathbf{s}}$.

The error correction involves three steps: estimating the number of erroneous coefficients, estimating the locations of those coefficients, and estimating the error values and decoding the message.

5.1. Estimation of the number of channel errors

We assume that the quantization noise \mathbf{q} is white and is uncorrelated with the channel errors. Each component of \mathbf{q} is assumed to have mean zero and variance σ^2 . The channel error magnitudes are assumed to be large compared to σ^2 .

Consider the modified syndrome coefficient matrix \hat{S} . Let S_e and S_q denote the parts due to the channel error and the

quantization noise, respectively, that is, $\hat{S} = S_e + S_q$. Therefore the syndrome covariance matrix is given as

$$\hat{R} = R + \frac{1}{d-l} (S_q S_q^h + S_e S_e^h + S_q S_e^h) \equiv R + R_n, \quad (36)$$

where R_n denotes the quantization noise term on the right-hand side. The presence of R_n will perturb the eigenvectors and the eigenvalues of R . The statistical behaviour of this perturbation depends on the statistical properties of R_n . Since \mathbf{q} is assumed to be uncorrelated with \mathbf{e} , $\mathbb{E}(S_e S_q^h) = \mathbb{E}(S_q S_e^h) = \mathbf{0}$, where \mathbb{E} denotes the mathematical expectation operator. Further, since \mathbf{q} is white and has variance σ^2 , it is easy to prove that $\mathbb{E}(S_q S_q^h) = \sigma^2 T T^h$, where T is a $(l+1) \times N$ full row-rank matrix whose elements are functions of elements of X and U .

Let the eigendecomposition of $T T^h$ be given as

$$T T^h = U_c \Delta_c U_c^h, \quad (37)$$

where U_c denotes the matrix of eigenvectors and Δ_c denotes the diagonal matrix of eigenvalues. Since $T T^h$ is positive-definite and Hermitian, all its eigenvalues are real and positive. Let $\Delta_c^{1/2}$ denote the diagonal matrix with the square roots of the eigenvalues on the diagonal, and let $\Delta_c^{-1/2}$ denote its inverse. Then premultiplying and postmultiplying (36) by $\Delta_c^{-1/2} U_c^h$ and $U_c \Delta_c^{-1/2}$, respectively, we obtain

$$\hat{R}_w = R_w + R_{wn}, \quad (38)$$

where $\hat{R}_w \equiv \Delta_c^{-1/2} U_c^h \hat{R} U_c \Delta_c^{-1/2}$, $R_w \equiv \Delta_c^{-1/2} U_c^h R U_c \Delta_c^{-1/2}$, and R_{wn} denotes the quantization noise term on the right-hand side. It is easy to see that $\mathbb{E}(R_{wn}) = \sigma^2 I_{l+1}$. If $\lambda_1 \geq \lambda_2 \geq \dots \geq \lambda_\nu$ are the nonzero eigenvalues of R_w , then the expected eigenvalues of \hat{R}_w are $\lambda_1 + \sigma^2 \geq \lambda_2 + \sigma^2 \geq \dots \geq \lambda_\nu + \sigma^2, \sigma^2, \dots, \sigma^2$. Since the channel errors are assumed to be large compared to the quantization step size, λ_i 's are relatively large compared to σ^2 . Therefore the number of errors can be estimated by using a threshold as is done for DFT codes in [7]. Observe that the transformation from \hat{R} to \hat{R}_w is required because of the generalized structure of the code. In the case of DFT codes, this is not required since $\mathbb{E}(S_q S_q^h) = \sigma^2 (d-l) I_{l+1}$ [12].

5.2. Estimation of error locations

5.2.1. Coding-theoretic approach

With quantization, the set of equations (30) no longer holds; each equation contains a noise term on the right-hand side. The coefficients of the error locator polynomial can be estimated from these equations by solving them in the least square sense using the pseudoinverse operator. The locations of the errors can be estimated by computing $|\hat{\Lambda}(x)|^2$, the squared magnitude of $\hat{\Lambda}(x)$, at $f(i)$, $i = 0, \dots, N-1$, and then finding the ν indices which give the minimum values. The above method is similar to the method applied to localize errors in quantized DFT codes [12], but the difference here is that the minimization of $|\hat{\Lambda}(x)|^2$ is over the range of function f .

5.2.2. Subspace approach

Consider (38). The rank of R_w is equal to the rank of R , that is, ν , and hence it has ν nonzero eigenvalues. The eigenvectors of R_w corresponding to the nonzero eigenvalues span the same subspace as spanned by the columns of $\Delta_c^{-1/2} U_c^h U_e$. This subspace is also spanned by the columns of $\Delta_c^{-1/2} U_c^h V_e$ since the columns of U_e and V_e span the same subspace. The eigendecomposition of \hat{R}_w gives

$$\hat{R}_w = [\hat{U}_{we} \ \hat{U}_{wn}] \begin{bmatrix} \hat{\Delta}_{we}^{\nu \times \nu} & \mathbf{0} \\ \mathbf{0} & \hat{\Delta}_{wn}^{(l+1-\nu) \times (l+1-\nu)} \end{bmatrix} [\hat{U}_{we} \ \hat{U}_{wn}]^h, \quad (39)$$

where $\hat{\Delta}_{we}$ contains the ν largest eigenvalues. The columns of \hat{U}_{we} span the subspace which is an estimate of the subspace spanned by the columns of $\Delta_c^{-1/2} U_c^h V_e$, and the columns of \hat{U}_{wn} span its orthogonal complement. Thus the errors can be localized by minimizing the following function over $f(i)$, $i = 0, \dots, N-1$:

$$\hat{E}(x) \equiv \mathbf{v}_x^h U_c \Delta_c^{-1/2} \hat{U}_{wn} \hat{U}_{wn}^h \Delta_c^{-1/2} U_c^h \mathbf{v}_x, \quad (40)$$

where $\mathbf{v}_x \equiv [1, x, x^2, \dots, x^l]^t$. Observe that the objective function $\hat{E}(x)$ defined above is different from that applied to quantized DFT codes [12] because of the generalized structure of the code.

Earlier we have mentioned that, when there is no quantization, the $(l+1)$ -dimensional vector consisting of the error locator polynomial coefficients, that is, Λ_l , lies in the noise subspace and has the minimum norm. This may not be true any longer when the coefficients are quantized, that is, the estimated vector $\hat{\Lambda}_l$ may not lie in the estimated noise subspace. Hence, the two approaches may not result in identical estimations of error locations. Because of the higher degrees of freedom, the perturbations of the subspaces will be less compared to the perturbation of Λ_l , and hence, the subspace approach is expected to result in more accurate estimations.

5.3. Message reconstruction

Once the erroneous coefficients are identified, there are two ways to reconstruct the message vector [8]. One obvious way is to decode the message vector directly from the uncorrupted received coefficients using frame-theoretic principles. If \mathbf{r}_R denotes the vector of uncorrupted received coefficients, and G_R denotes the set of rows of frame operator G corresponding to those coefficients, then the message can be decoded as $\hat{\mathbf{x}} = (G_R^h G_R)^{-1} G_R^h \mathbf{r}_R$. The other way is to decode the errors in the corrupted coefficients using the coding-theoretic principles. When the coefficients are quantized, the syndrome equations in (23) are no longer satisfied; each equation contains a noise term on the right-hand side. The error values can be estimated by solving them in the least square sense. The message vector can be estimated by first subtracting the decoded error values from the corrupted coefficients, and then applying the dual frame operator to all the coefficients. If $\hat{\mathbf{y}}$ denotes the vector of coef-

TABLE 1: SNR (dB) for different numbers of erasures.

No. of erasures	DFT	DCT	DST
0	31.80	31.80	31.80
1	31.23	31.05	31.19
2	30.45	29.57	30.28
3	29.27	25.07	28.61
4	27.16	10.76	23.00
5	23.14	-1.64	6.99
6	15.19	-21.25	-14.74
7	2.64	-46.69	-41.84

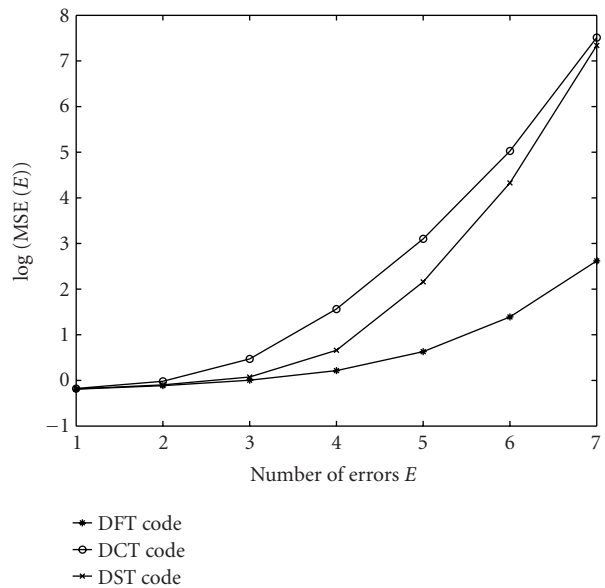


FIGURE 1: Average MSE for different numbers of erasures.

ficients after error correction, then the message vector can be estimated as $\hat{\mathbf{x}} = (G^h G)^{-1} G^h \hat{\mathbf{y}}$. It can be shown that both approaches result in the same reconstruction [8]. In addition, in either case, the mean square reconstruction error is equal to $(\sigma^2/K) \text{tr}((G_R^h G_R)^{-1})$, where $\text{tr}(\cdot)$ denotes the trace of a matrix and σ^2 is the variance of the quantization noise [4].

6. SIMULATION RESULTS

We performed simulations with a Gauss-Markov source with mean 0, variance 1, and correlation coefficient 0.9. The source was divided into blocks of length 9 (K), and each block was expanded to 16 (N) coefficients using frames associated with $(16, 9)$ lowpass DFT, DCT, and DST codes. The expansion coefficients were quantized with a 4-bit uniform scalar quantizer.

First we considered only erasures of coefficients. With a $(16, 9)$ -BCH-like complex code, up to 7 erasures can be recovered. Table 1 displays the average signal-to-noise ratio (SNR) for different numbers of erasures. Figure 1 shows the theoretical mean square error (MSE) for different numbers

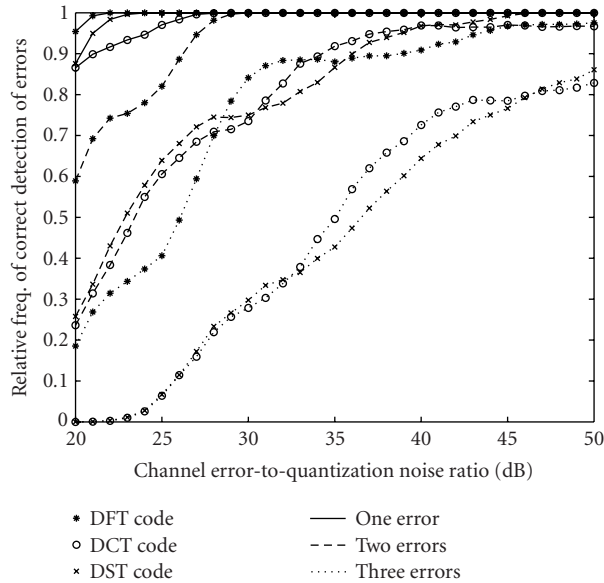


FIGURE 2: Relative frequency of correct detection of errors at different channel error-to-quantization noise ratios.

of erasures with σ^2 normalized to 1. The theoretical MSE values are computed by computing mean square reconstruction errors for all possible erasure patterns for a given number of erasures and then taking the average of them. Both results show that the frame expansion with the DFT code performs the best and that with the DCT code performs the worst. This is a result of the fact that, for DFT codes, the frames associated with the received coefficients have closer bounds than those associated with the DCT and the DST codes. The observation that the MSE increases with the increase in the number of erasures is characteristic of quantized frame expansions.

Then we considered coefficient errors with varying channel error to quantization noise ratio. In the first step, we considered only the coding-theoretic approach to error localization and compared the performances of the frames associated with lowpass DFT, DCT, and DST codes. With a (16, 9)-BCH-like complex code, up to three errors can be corrected. For a given number of errors, the locations of the erroneous coefficients were chosen randomly. Figure 2 shows the relative frequency of the correct number of estimated errors. Figure 3 shows the relative frequency of the correct localization of errors assuming that the number of errors is estimated correctly. We observe that, in both steps, the frame expansion by the DFT code outperforms those by the DCT and the DST codes. When there is no quantization noise, the roots of the error locator polynomial for the DFT code are distinct N th roots of unity and they all lie on the unit circle. In the case of the DCT and the DST codes, the roots are all real and distinct. When there is quantization, the roots for the DFT code lie about the unit circle whereas, in the case of the DCT and the DST codes, the roots can be real or complex conjugate pairs. Recall that the errors are localized by minimizing the absolute square of the estimated locator polynomial over the

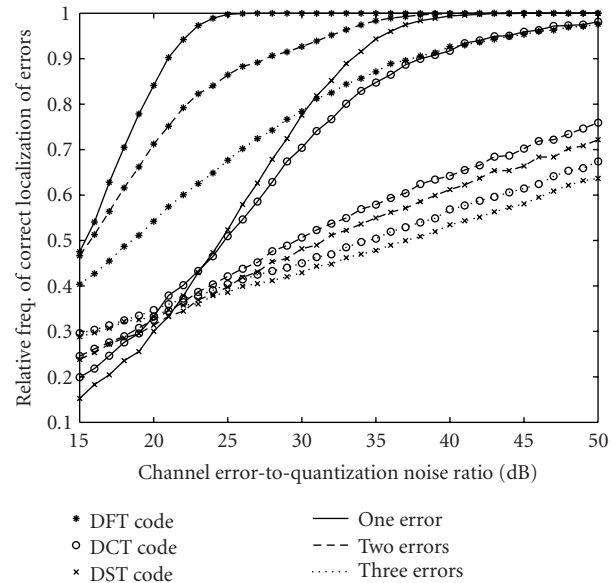


FIGURE 3: Relative frequency of correct localization of errors at different channel error-to-quantization noise ratios.

range of function f . It is easy to see that the roots for the DFT code have more degrees of freedom for perturbation than those for the DCT and the DST codes. Thus the DFT code is expected to result in better localization results.

In the second step, we compared the error localization efficiencies of the coding-theoretic and the subspace decoding approaches. The same Gauss-Markov source was expanded with the frames associated with the (18, 9) lowpass DFT, DCT, and DST codes. With a (18, 9)-BCH-like complex code, up to four errors can be corrected. Figures 4 and 5 show the relative frequency of correct localization of one and two errors, respectively. The performance improvement of the subspace algorithm over the locator polynomial approach is clear from the displayed figures. We have observed that the performance improvement decreases as the number of errors is increased. When the number of errors is equal to 4, the performances of the two approaches are similar. This is expected because, as the number of errors is increased, the dimension of the noise subspace is decreased, and when the number of errors is equal to 4, the noise subspace has dimension one. Higher noise subspace dimensionality provides greater degrees of freedom and thus lesser perturbations for the noise subspace. The plots also show that the DFT code outperforms both the DCT and the DST codes. The better performance of the DFT code is once again because of the similar reason as stated in the previous paragraph.

Finally, we applied the lowpass DFT, DCT, and DST frame expansions to the Lena image (grayscale, 512×512). The image was divided into blocks of size 8×8 , and the DCT was applied to each block. Transform coefficients associated with the same frequency from 8 consecutive blocks were expanded to 16 coefficients using the (16, 8) lowpass DFT, DCT, and DST frames. The coefficients were quantized using a uniform quantizer having step size 16 and then fixed-length

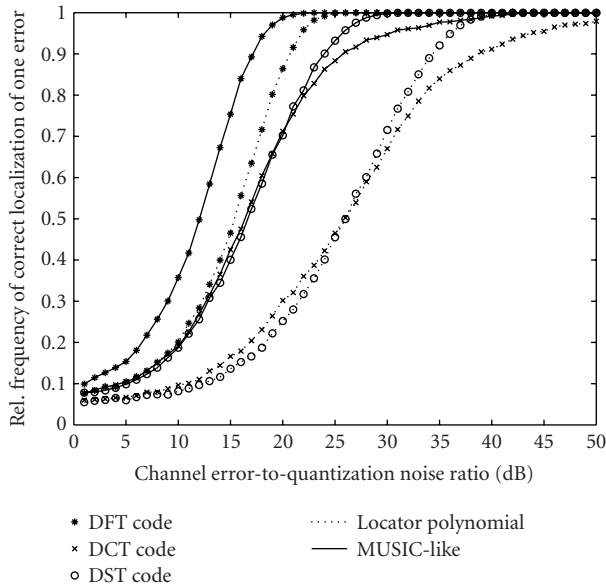


FIGURE 4: Relative frequency of correct localization of one error at different channel error-to-quantization noise ratios.

encoded using 8 bits. This process was applied only to the lowest ten frequency coefficients of each block. The remaining frequency coefficients were quantized to zero. During the decoding, we assumed that the number of coefficient errors in a frame expansion was known.

Table 2 shows the PSNR of the reconstructed image at different channel bit error rates (BERs) for both the coding-theoretic and the subspace-based error localizations. The results are averaged over the same 20 channel realizations for the three frames. We observe that, at very low BERs, the performances of the three frames are similar. At higher BERs, the DFT frame performs better than both the DCT and the DST frames with coding-theoretic localization; however, when the errors are localized using the subspace approach, surprisingly, the DCT and the DST frames perform better than the DFT frame. This could happen perhaps because of the large quantization step size, which makes the error localization inefficient for larger number of errors. Moreover, this is appropriate to note here that, correct error localization does not necessarily lead to the least reconstruction error. The SNR of the reconstructed message depends on the number of the erroneous coefficients as well as their locations [4, 8]. The performance improvement of the subspace approach over the coding-theoretic approach is evident from the two tables. Figure 6 displays the reconstructed images at BER 0.001 for one channel realization. We observe that the quality of the reconstructed image is better with the subspace-based error localization.

7. CONCLUSION

In this paper, we have characterized a class of finite frames which can be considered for joint source-channel coding in cross-layer-enabled wireless communication environments.

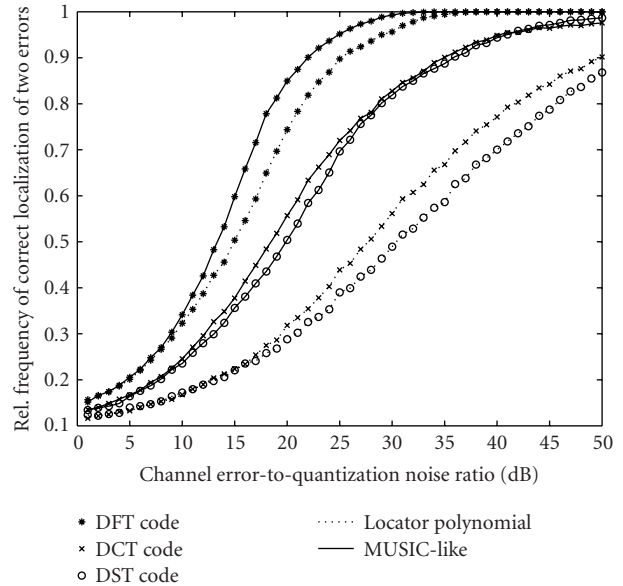


FIGURE 5: Relative frequency of correct localization of two errors at different channel error-to-quantization noise ratios.

TABLE 2: PSNR for Lena image for different frames at different bit error rates. (a) Error localization by coding-theoretic approach. (b) Error localization by subspace approach.

(a)				
BER 10^{-4}	5×10^{-4}	10^{-3}	5×10^{-3}	10^{-2}
DFT 31.89	31.60	31.17	24.59	19.27
DCT 31.78	31.29	30.46	23.32	18.07
DST 31.86	31.48	30.87	23.43	18.06
(b)				
BER 10^{-4}	5×10^{-4}	10^{-3}	5×10^{-3}	10^{-2}
DFT 31.90	31.83	31.50	26.43	20.45
DCT 31.89	31.82	31.75	28.36	21.80
DST 31.90	31.88	31.81	28.64	21.92

Evolving at the application layer, they allow for error correction besides erasure recovery. We have associated the frames with complex number codes and characterized them based on the BCH-like properties of the parity check matrices of the associated codes. In particular, we have considered the frames associated with the lowpass DFT, DCT, and DST codes, which are shown to belong to this class. Besides the standard BCH-like decoding approach, we have also presented a subspace-based algorithm for localizing the errors in the frame expansion coefficients. We have compared the performance of the subspace algorithm with the BCH decoding approach for the lowpass DFT, DCT, and DST frame expansions. Simulation results show that the subspace algorithm can improve the error localization accuracy with quantized frame expansions, especially at fewer number of



FIGURE 6: Reconstructed image with BER 0.001. (a) Error localization with coding-theoretic approach for DFT frame, DCT frame, and DST frame (from left to right). (b) Error localization with subspace approach for DFT frame, DCT frame, and DST frame (from left to right).

coefficient errors. Among the lowpass DFT, DCT, and DST frames, the DFT frame has the best performance with a Gauss-Markov source. When the subspace algorithm is applied for image transmission, the DCT and DST frames are observed to perform better than the DFT frame at high BERs.

Utilization of frames for robust multimedia transmission is relatively new. In that context, this paper has considered only a class of frames and demonstrated their use in digital communication. It is now clear that all frames belonging to the same class do not result in the same reconstruction error even though they are all tight. Thus finding the best frames in the sense of minimum reconstruction error and numerical stability is an open issue. Further, this paper has considered only frames in \mathbb{C}^K and \mathbb{R}^K . Use of frames in $\ell^2(\mathbb{Z})$ for correcting errors in message sequences is a much more challenging problem.

REFERENCES

- [1] C. Bormann, C. Burmeister, M. Degermark, et al., "Robust Header Compression (ROHC): Framework and four profiles: RTP, UDP, ESP, and uncompressed," IETF RFC 3095, July 2001.
- [2] L.-A. Larzon, M. Degermark, and S. Pink, "The UDP-Lite Protocol," IETF Internet Draft, December 2002, <http://www.ietf.org/proceedings/03jul/I-D/draft-ietf-tsvwg-udp-lite-01.txt>.
- [3] A. C. Lozano, J. Kovačević, and M. Andrews, "Quantized frame expansions in a wireless environment," in *Proc. Data Compression Conference (DCC '02)*, pp. 232–241, Snowbird, Utah, USA, April 2002.
- [4] V. K. Goyal, J. Kovačević, and J. A. Kelner, "Quantized frame expansions with erasures," *Applied and Computational Harmonic Analysis*, vol. 10, no. 3, pp. 203–233, 2001.
- [5] R. E. Blahut, *Algebraic Methods for Signal Processing and Communications Coding*, Springer-Verlag, New York, NY, USA, 1992.
- [6] T. G. Marshall Jr., "Coding of real-number sequences for error correction: a digital signal processing problem," *IEEE Journal on Selected Areas in Communications*, vol. 2, no. 2, pp. 381–392, 1984.
- [7] A. Gabay, P. Duhamel, and O. Rioul, "Spectral interpolation coder for impulse noise cancellation over a binary symmetric channel," in *Proc. European Signal Processing Conference (EUSIPCO '00)*, Tampere, Finland, September 2000.
- [8] G. Rath, X. Henocq, and C. Guillemot, "Application of DFT codes for robustness to erasures," in *IEEE Global Telecommunications Conference (GLOBECOM '01)*, pp. 1246–1250, San Antonio, Tex, USA, September 2001.
- [9] J.-L. Wu and J. Shiu, "Real-valued error control coding by using DCT," *IEEE Proceedings Part I: Communications, Speech and Vision*, vol. 139, no. 2, pp. 133–139, 1992.
- [10] S. Haykin, *Adaptive Filter Theory*, Prentice-Hall, Englewood Cliffs, NJ, USA, 1991.
- [11] S. M. Kay, *Modern Spectral Estimation: Theory and Application*, Prentice-Hall, Englewood Cliffs, NJ, USA, 1988.
- [12] G. Rath and C. Guillemot, "Subspace algorithms for error localization with DFT codes," in *Proc. IEEE Int. Conf. Acoustics, Speech, Signal Processing (ICASSP '03)*, vol. 4, pp. 257–260, Hong Kong, China, April 2003.
- [13] I. Daubechies, *Ten Lectures on Wavelets*, Society for Industrial and Applied Mathematics (SIAM), Philadelphia, Pa, USA, 1992.
- [14] A. Gabay, P. Duhamel, and O. Rioul, "Real BCH codes as joint source channel codes for satellite image coding," in *Proc. IEEE Global Telecommunications Conference (GLOBECOM '00)*, pp. 820–824, San Francisco, Calif, USA, November–December 2000.
- [15] O. Rioul, "A spectral algorithm for removing salt and pepper from images," in *Proc. IEEE Workshop on Digital Signal Processing*, pp. 275–278, Loen, Norway, September 1996.

- [16] M. R. Spiegel and J. Liu, *Mathematical Handbook of Formulas and Tables*, Schaum's Outline Series. McGraw-Hill, New York, NY, USA, 2nd edition, 1998.
- [17] R. E. Blahut, *Theory and Practice of Error Control Codes*, Addison-Wesley, Reading, Mass, USA, 1983.
- [18] P. J. S. G. Ferreira and J. M. N. Vieira, "Locating and correcting errors in images," in *Proc. 4th IEEE International Conference on Image Processing (ICIP '97)*, vol. 1, pp. 691–694, Santa Barbara, Calif, USA, October 1997.
-

Gagan Rath received the B.Tech. degree in electronics and electrical communication engineering from the Indian Institute of Technology Kharagpur in 1990, and the M.E. and Ph.D. degrees in electrical communication engineering from the Indian Institute of Science, Bangalore, in 1993 and 1999. He is currently working as a Research Scientist at INRIA, France. His research interests are in broadly digital signal processing and communications.



Christine Guillemot is currently "Directeur de Recherche" at INRIA, in charge of a research group dealing with image modelling, processing, and video communication. She holds a Ph.D. degree from ENST (École Nationale Supérieure des Télécommunications), Paris. From 1985 to October 1997, she was with France Telecom/CNET, where she was involved in various projects in the domain of coding for TV, HDTV, and multimedia applications. From January 1990 to mid 1991, she worked at Bellcore, NJ, USA, as a Visiting Scientist. Her research interests are in signal and image processing, video coding, and joint source and channel coding for video transmission over the Internet and over wireless networks. She currently serves as an Associated Editor for IEEE Transactions on Image Processing.

